DOI 10.1007/s10891-019-02014-5
Journal of Engineering Physics and Thermophysics, Vol. 92, No. 4, July, 2019

INFLUENCE OF THE MANIFOLD CONFIGURATION OF PULSATING HEAT PIPES ON THEIR PERFORMANCE

B. Agostini, D. Torresin, and M. Bortolato UDC 536.248.2

The performance characteristics of three air-to-air pulsating heat pipes with R1233zd as a working fluid for cooling an electronic cabinet are presented. Each of these pipes comprises two coolers staked in one unit of dimension 36 × 19 × 5 cm^3, constructed with extruded multiport tubes and louvered fins brazed together. These pipes differ from each other only in their manifold configuration achieved by having fluid distribution plates at the evaporator and condenser manifolds to provide a serial connection of the flow paths. The experiments were performed with PHPs of only one type, composed of two coolers in stack and turned through 90^o on their narrow side. A new parameter, representing the rate of pressure pulsations in a PHP, was introduced into consideration, and it is shown that this parameter correlates with the PHP performance.

Keywords: *pulsating heat pipe, two-phase flow, electronic cabinet, cooling.*

Introduction. Outdoor cabinets including power electronic components need effective cooling. At the same time, they should be protected from the outside air, which can contain moisture, and dirt, which would reduce the reliability of the electronics. In this case, water cooling is the most effective cooling method. However, water is often undesirable because of high voltages or customer requirements. The mark of power electronics is expanding to the regions of the world where the air temperature can decrease to –60°C (e.g., in Siberia) or increase to 60°C (e.g., in the Middle East), and water (and its glycol mixtures) can freeze or are not available onsite. In order to provide the required performance at a low cost with air cooling, the ABB patented a pulsating heat-pipe cooler, developed by Fabbri and Agostini [1], which is based on the automatic compact heat-exchanger technology (Fig. 1).

A pulsating heat pipe (PHP) has been devised in the early 90s by Akachi [2, 3]. In such a pipe, heat is transferred due to the pulsations of the liquid slugs and elongated bubbles in the space between the evaporator and the condenser. Pulsating heat pipes, which are analogous to thermosyphons, are cheap because of the absence of a wick structure in them; they are compact, and entirely passive with the advantage of operating independently of their orientation, allowing high flexibility in the case of their mechanical integration. In spite of the significant recent experimental and theoretical efforts made towards PHPs, a number of problems on the mechanism of operation of a PHP remain to be solved. Pulsating heat pipes with the above indicated advantages, as compared to conventional heat pipe systems, are considered an interesting alternative to modern heat exchangers [4]. However, because of the complicated thermal and hydrodynamic conditions of operation of such pipes, the PHP technologies are not yet widespread.

According to the literature data, the main application of pulsating air to air heat exchangers is for heat recovery systems. In [5], the feasibility of using a pulsating finned heat pipe (PFHP), filled with acetone, for the heat exchange between the counter air flows in a HVAC air system was investigated. The data on the heat transfer and the pressure drop in such pipes, obtained in this work, show that a PFHP of height 122 cm, width 46 cm, and depth 46 cm has an efficiency of the order of 0.48 with a pressure drop of about 40 Pa at $T_{hi} - T_{ci} = 17$ K, resulting in the pre-cooling of the incoming air by 8 K. In [6], an experimental prototype of an air preheater, representing a pulsating closed-ended heat pipe (PCEHP), has been designed and fabricated for investigating the applicability of such a heater as a waste-heat recovery device for a drying process. A PCEHP of height 38 cm, width 20 cm, and depth 80 cm with R123 as a working fluid has an efficiency of 0.44 at $T_{hi} - T_{ci} = 30$ K with no pressure drop. The authors of the indicated works concluded that pulsating air-to-air heat exchangers are suitable for heat-recovery applications.

ABB Switzerland Ltd., Corporate Research Segelhofstrasse 1K, CH-5405 BADEN-DAETTWIL, Switzerland; email: bruno.agostini@ch.abb.com. Published in Inzhenerno-Fizicheskii Zhurnal, Vol. 92, No. 4, pp. 1042–1049, July–August, 2019. Original article submitted December 11, 2018.

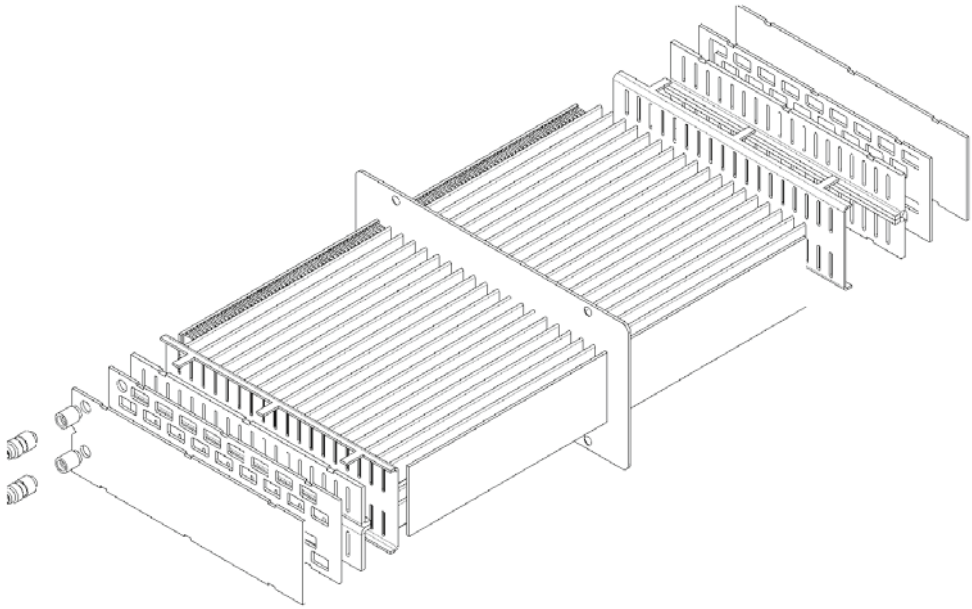

Fig. 1. Manifold configuration of a pulsating heat pipe.

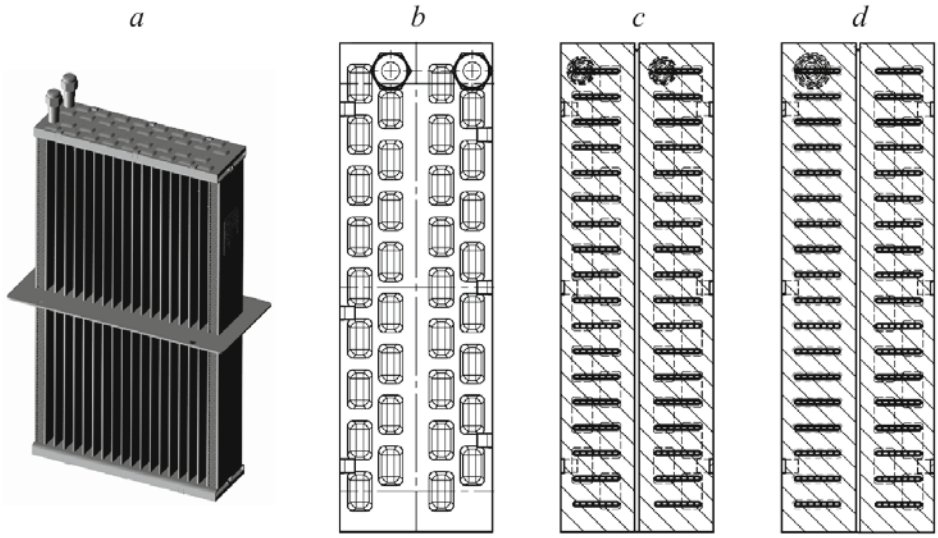

Fig. 2. 3D view of a pulsating heat pipe (a) and its EMB (b), FLAT-S (c), and FLAT-U (d) manifold configurations.

The present work is a continuation of the works [7, 8]. Three pulsating heat pipes having the FLAT-S, EMB, and FLAT-U manifold configurations (Table 1) have been constructed using the fluid distribution plates of different types (Fig. 2). The design of these PHPs is based on the concept developed at the ABB [1] for pulsating open-loop heat pipes (POLHP). In the FLAT-S pipe, the plate installed at the condenser manifold provides, due to its cut-outs, the distribution of the fluid in the pipe so that the fluid coming from the group of channels of the first extruded multiport tube (EMPT) is directed to the group of channels of the adjacent second EMPT, and so on. The plate installed at the evaporator manifold is an antisymmetric projection of the condenser plate, and it provides the same fluid distribution but offset by one EMPT. A plain plate is brazed at the top of the system to close it hermetically. The flow path realized in the EMB pipe is similar to that in the FLAT-U pipe, but it is provided by the embossment of a fluid distribution plate rather than by its cut-outs, and no closing plate is required in this pipe. In the FLAT-U pipe, a fluid distribution plate similar to that of the FLAT-S pipe is installed at the condenser manifold, and the evaporator EMPTs each have U-turns at their top.

TABLE 1. Manifold Configurations and Dimensions of the Tested Prototypes

Pipe	FLAT-S	EMB	FLAT-U
Height	358 mm	358 mm	358 mm
Width	192 mm	192 mm	192 mm
Depth	50 mm	50 mm	50 mm
EMPT	2×18 mm^2	2×18 mm^2	2×18 mm^2
Fluid channels	2.16×1.2 mm^2	2.16×1.2 mm^2	2.16×1.2 mm^2
Number of channels/EMPT	7	7	7
Fin height	8 mm	8 mm	8 mm
Fin pitch	3 mm	3 mm	3 mm
Evaporator height	165 mm	165 mm	161 mm
Evaporator manifold height	13.5 mm	13.5 mm	17.5 mm
Evaporator distribution	square openings	embossed plate	U turns
Condenser height	164 mm	164 mm	164 mm
Condenser manifold height	13.5 mm	13.5 mm	13.5 mm
Condenser distribution	square openings	embossed plate	square openings

Experimental Setup. A block diagram of the experimental setup is shown in Fig. 3. This setup comprises a PHP with an absolute-pressure sensor and a fluid thermocouple at the evaporator manifold, two counterflow air tunnels each with a centrifugal fan, a sensor and a preheater of an air flow, two inlet air distribution cones with a thermocouple and an air-pressure measurement port, two outlet air cones each with a thermocouple and an air-pressure measurement port, and two differential air-pressure sensors.

All the signals are acquired through the National Instruments SCXI connected to a laptop running LabVIEW®. For pressure measurements, the SCXI box is equipped with a 1102C acquisition module recording signals at a frequency of 10 kHz. For temperature measurements, a 1102 module with a cut-off frequency of 2 Hz is used. All the thermocouples were calibrated using an Omega DP97 precision thermometer with platinum probes as the reference temperature and a Lauda R207 chiller to control the temperature. The uncertainty of the calibrated thermocouples was ± 0.1 K. The measuring devices and their accuracy are presented in Table 2. The internal pressure and temperature of the fluid flowing through the filling port of a pipe were measured with the use of a pressure and a temperature sensor. Since the pipes being considered comprise two coolers stacked in one unit, air flows through both of them, but the internal fluid circulations are realized in these coolers independently, and each of them can be filled separately. We present experimental data obtained for the PHPs of only one type, composed of two coolers in stack and turned through 90° on their narrow side. In all the pipes, R1233zd was used as a working fluid.

Data Reduction. Different parameters of a PHP need analysis. The fill ratio of the PHP has the form

$$F_{\mathrm{r}} = m_{\mathrm{f}}/(\rho_{\mathrm{f}} V) \,, \tag{1}$$

where ρ_{f} is the density of the fluid, m_{f} is the volume (mass) of the fluid filling the PHP, and V is its internal volume. The heat capacity rate of the air in the PHP is determined from the expression

$$C_{\mathrm{a}} = \dot{m}_{\mathrm{a}} c_{p\mathrm{a}} \,, \tag{2}$$

where $c_{p\mathrm{a}}$ is the specific heat capacity of the air in the PHP estimated at its average temperature. The heat capacity ratio of the PHP has the form

$$C_{\mathrm{r}} = C_{\mathrm{c}}/C_{\mathrm{h}} \,, \tag{3}$$

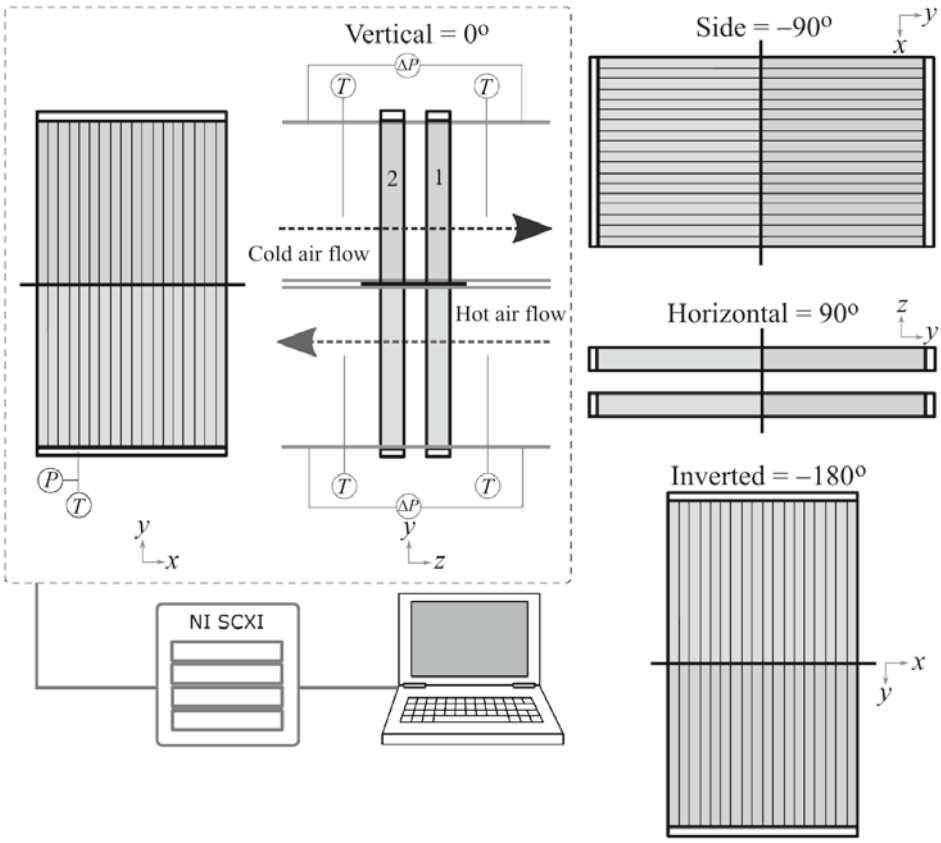

Fig. 3. Block diagram of the experimental setup.

TABLE 2. Measuring Devices and Accuracy

Measurement	Device	Measurement range	Accuracy
Temperatures	type K, diameter 1 mm	25–90°C	± 0.1°C
Evaporator pressure	Omega PX409	0–17.5 bar	± 0.02 bar
Hot air flow	ABB SensyFlow P	80–4000 kg/h	± 4 kg/h
Cold air flow	TROX VMR-250	216–2214 kg/h	± 5%

where C_c and C_h are the heat capacities of the air at the condenser and evaporator sides. The minimum heat capacity of the air in the PHP is defined as

$$C_{min} = \min(C_c, C_h) . \quad (4)$$

Finally, the efficiency of the PHP is determined from the expression

$$\eta = C_h/C_{min}(T_{hi} - T_{ho})/(T_{hi} - T_{ci}) = Q/Q_{max} , \quad (5)$$

representing the ratio between the actual rate of heat transfer in the PHP and the maximum possible rate of heat transfer attained in an infinite PHP. The efficiency of air-to-air heat exchangers is traditionally considered as an indicator of their performance.

Comparison of the Performance Characteristics of PHPs Having Different Manifold Configurations. The influence of the fill ratio of a PHP on its heat load changes when the vertical orientation of the PHP changes to the side one, and this effect is not the same for the PHPs being investigated.

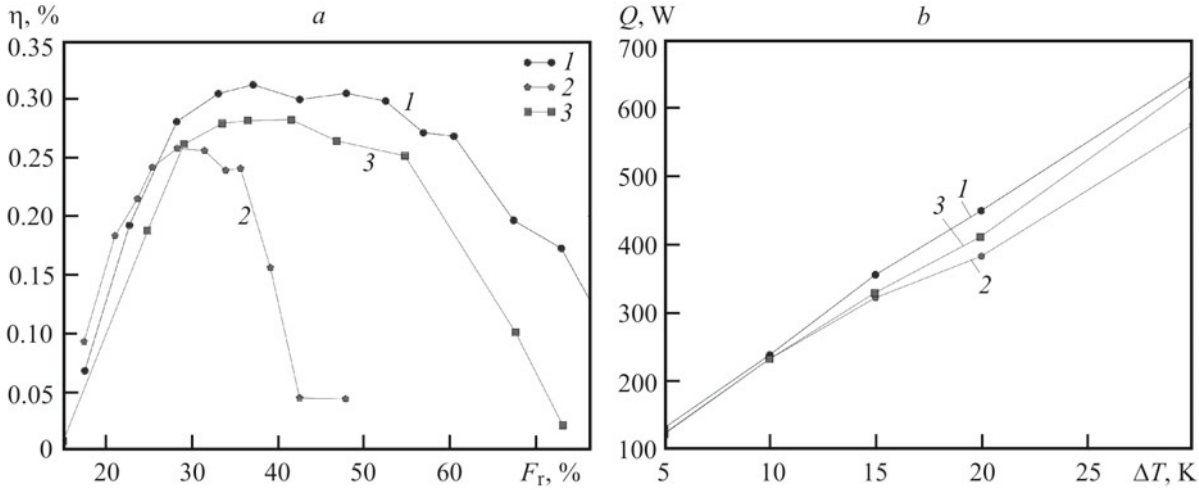

Fig. 4. Efficiency of the FLAT-U (1), EMB (2), and FLAT-S pipes (3) vs. their fill ratio at $\Delta T = T_{hi} - T_{ci} = 20$ K (a) and heat load of these pipes vs. ΔT (b) at an air flow rate of 250 m^3/h and an inlet air temperature of 50°C: 1) $F_r = 37\%$; 2) 31; 3) 32.

Figure 4a shows the average efficiencies of three pipes of the FLAT-S, EMB, and FLAT-U manifold configurations versus their fill ratio at $T_{hi} - T_{ci} = 20$ K in the case of their side orientation (–90°). The side orientation is required for obtaining the final product. Because of this, we will focus on the measurements performed for this orientation. The fill-ratio range of the FLAT-U pipe is much wider than that of the other pipes. Actually, a heat load lower than 10% can be attained in it at a fill ratio ranging from 28 to 60%. For the FLAT-S pipe, this limited performance is possible in the case where its fill ratio falls within the range 25–40%, while the EMB pipe is able to maintain a good performance in the very narrow fill-ratio range 28–33%. An analysis of the entire data set collected for each pipe has shown that the optimum fill ratio of a PHP, corresponding to its maximum load by the heat dissipated in it is 37% for the FLAT-U pipe, 33% for the FLAT-S pipe, and 31% for the EMB pipe. Figure 4b shows the load of the three pipes being considered by the heat transferred in them versus the maximum difference between the air temperatures T_{hi} and T_{ci} at an optimum fill ratio. The trend of change in the indicated load is linear for all the pipes; hence, the operating limits of the pipes with a side orientation, associated with the onset of the dry-out process, have not been attained during the experiments with them. The performance characteristics of the three pipes are very similar in the case where ΔT_{max} is as large as 10 K, and the maximum heat load is approximately equal to 235 W at $\Delta T_{max} = 10$ K. On the other hand, at $\Delta T_{max} = 20$ K, the maximum heat load of the FLAT-U pipe comprises 450 W, which is 10% and 17.5% higher than that of the FLAT-S pipe (410 W) and the EMB pipe (380 W), respectively. The superior performance provided by the FLAT-U manifold configuration can be due to the lower pressure drop in the U turns compared to that in the square cross opening. A proper measurement setup is required to confirm this hypothesis.

Pressure Pulsation Rate. Figure 5 shows a typical time series of fluid-pressure pulsations and the corresponding fast Fourier transform (FFT). Periodic pressure peaks are seen, and the Fourier transform yields the two peaks at approximately 0.65 and 1.5 Hz at this operation point. The maximum fundamental frequency of the pressure pulsations was 1.5 Hz and their amplitude was ± 0.5 bar. A system analysis of the data obtained in a definite period of time has shown that the variable pressure pulsation rate (PPR) is adequately defined by the equation

$$u = \langle f \rangle \langle \Delta P \rangle , \tag{6}$$

where $\langle f \rangle$ is the average frequency of the pressure pulsations in this time period, and $\langle \Delta P \rangle$ is the average value of these pulsations. A typical plot of the rate of pressure pulsations in a PHP versus the temperature difference between the hot and cold air flows in it is shown in Fig. 6 for the FLAT-S and FLAT-U pipes, and curves of the heat load of these pipe under the same experimental condition are also presented here. Figure 7 presents the heat load and the pressure pulsation rate of these pipes as functions of their fill ratio. These graphs show that the performance of a PHP depends on the rate of pressure pulsations in it: the larger the heat load of the PHP, the higher the PPR. The approach proposed makes sense from the physical standpoint if one considers that, to obtain watts, one just need to multiply Pa/s by a volume. Therefore, the pumping power of a PHP at its operating point can be defined as

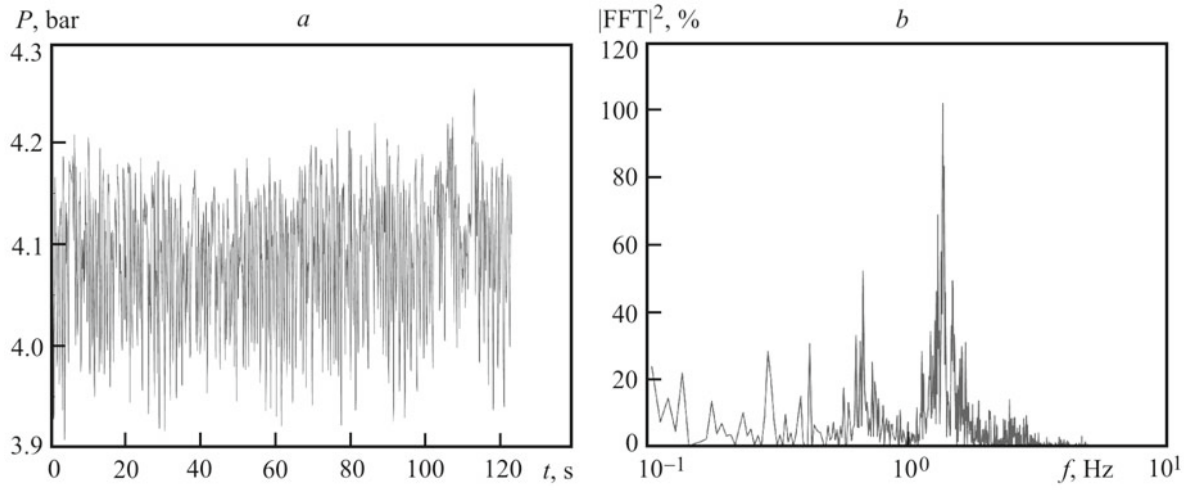

Fig. 5. Internal pressure of a FLAT pipe in the side position vs. the time (a) and corresponding FFT (b) at ΔT = 20 K, an air flow rate of 250 m^3/h, and an inlet air temperature of 50°C.

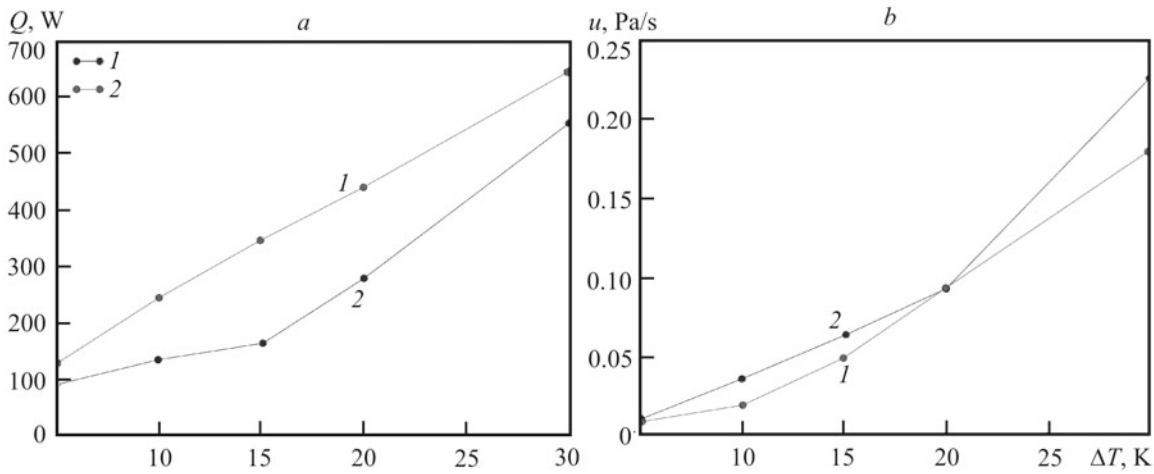

Fig. 6. Heat load (a) and pressure pulsation rate (b) vs. the temperature difference for the FLAT-S (1) and FLAT-U pipes (2) at an air flow rate of 250 m^3/h and an inlet air temperature of 50°C: 1) F_r = 25%; 2) 33.

$$W = \langle f \rangle \langle \Delta P \rangle V \varepsilon \,, \tag{7}$$

where V is the internal volume of the PHP and ε is the void fraction at its operating point. Unfortunately, the void fraction cannot be determined with the setup used in the present work since it is a function of the vapor quality and the internal fluid velocity.

The Pearson coefficient of correlation between the heat load of a PHP and the rate of pressure pulsations in it was calculated for the FLAT-S pipe, and it was about 0.86 for a set of 135 data points, which points to a good correlation between the indicated parameters, as illustrated in Fig. 8. Therefore, it may be suggested that the performance of a PHP is physically related to the rate and value of pressure pulsations in it, so that the performance of the PHP is strongly dependent on the product of the amplitude of the pressure pulsations in it into their frequency. In spite of the high correlation coefficient of the data obtained, their scatter is significant. We hypothesize that this scatter can be decreased with the use of the void fraction term involved in Eq. (7).

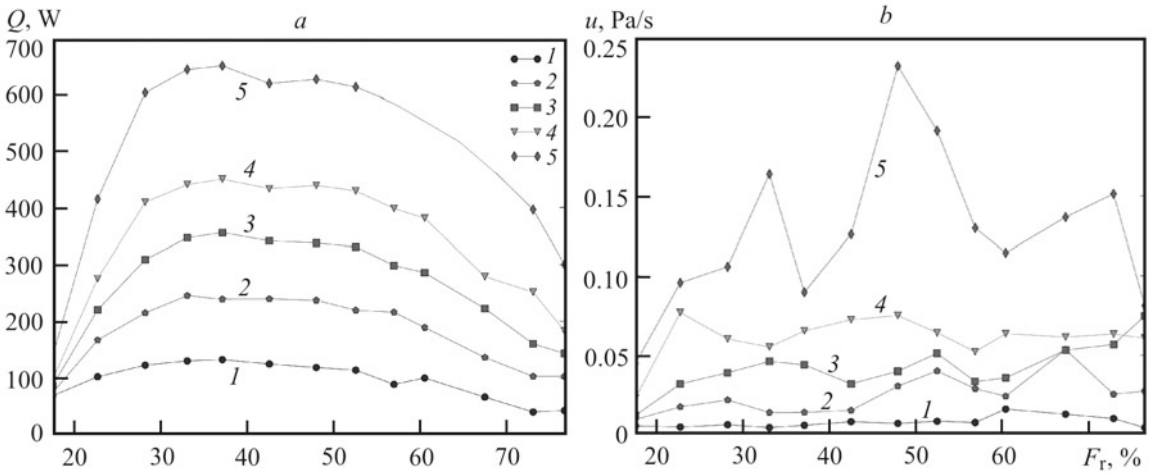

Fig. 7. Heat load (a) and pressure pulsation rate (b) vs. the fill ratio at various temperature differences for the FLAT-S pipe at an air flow rate of 250 m^3/h and an inlet air temperature of 50°C: 1) ΔT = 5 K; 2) 10; 3) 15; 4) 20; 5) 30.

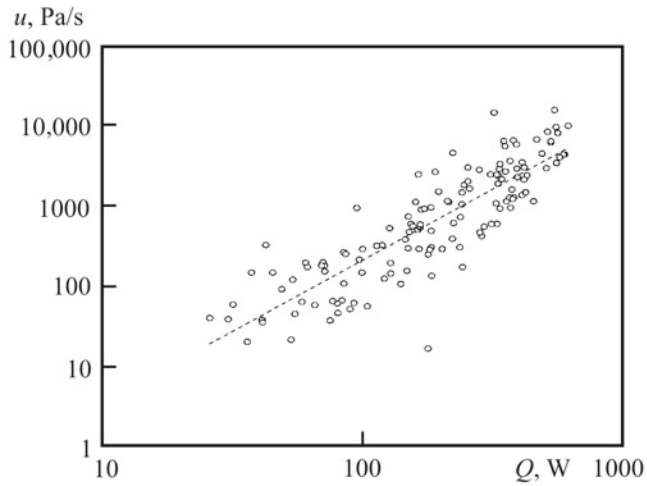

Fig. 8. Pressure pulsation rate vs. the heat load of the FLAT-S pipe.

Conclusions. The performance of the novel air-to-air pulsating heat pipe, based on the automatic heat-exchanger technology, was experimentally investigated with three its prototypes of different manifold configurations, in which R1233zd was used as a working fluid. It was established that a single-filled POLHP cooler with a volume of 2 L only possesses a 32% efficiency (it can dissipate a heat flow of power as high as 650 W at a maximum temperature difference between the hot and cold air flows of 30 K. A FLAT-U pipe, having U-turns at its hot side and a square cross opening at the cold side, is characterized by the best performance as regards the heat load and the optimal fluid filling range. The pressure loss in the PHP being investigated is 25 Pa, and its performance depends strongly on the product of the amplitude of pressure pulsations in it and their frequency.

A further work should investigate if the pressure pulsation rate concept can provide a path towards a semi-analytical method for prediction of the performances of pulsating heat pipes. Secondly, the use of a more accurate pressure sensor and a longer acquisition time may improve the accuracy of determining the rate of pressure pulsation in a PHP. Finally, an investigation to determine a manifold configuration of a PHP that would minimize the pressure losses in its turns should be conducted.

NOTATION

C, heat capacity rate, W/K; f, frequency, Hz; F_r, fill ratio, %; m, mass, kg; $\dot{m}$, mass flow rate, kg/s; P, pressure, Pa; ΔP, pressure difference, Pa; Q, heat load, W; T, temperature, °C; $\Delta T = T_{hi} - T_{ci}$, temperature difference, K; t, time, s;

u, pressure pulsation rate, Pa/s; *V*, volume, m^3; *W*, pumping power, W; η, efficiency, %; Subscripts: a, air; c, cold side; e, evaporator; f, fluid; h, hot side; i, inlet; min, minimum; max, maximum; o, outlet; r, ratio.

REFERENCES

1. B. Agostini and M. Fabbri, *Heat Exchanger Based on Pulsating Heat Pipe Principle,* European Patent No. 2444770 A1 (2012).
2. H. Akachi, F. Polasek, and P. Stulc, Pulsating heat pipes, in: *Proc. 5th Int. Heat Pipe Symp.*, Melbourne, Australia (1996), pp. 208–217.
3. H. Akachi, *Structure of a Heat Pipe*, US Patent No. 3229759 A (1998).
4. L. L. Vasiliev, Heat pipes in modern heat exchangers, *Appl. Therm. Eng.*, **25**, 1–19 (2005).
5. G. Mahajan, S. M. Thompson, and H. Cho, Energy and cost savings potential of oscillating heat pipes for waste heat recovery ventilation, *Energy Rep.*, **3**, 46–53 (2017).
6. S. Rittidech, W. Dangeton, and S. Soponronnarit, Closed-ended oscillating heat-pipe (CEOHP) air-preheater for energy thrift in a dryer, *Appl. Energy*, **81**, No. 2, 198–208 (2005).
7. M. Habert and B. Agostini, Pulsating air to air heat exchanger for enclosure cooling, in: *Proc. IX Minsk Int. Seminar "Heat Pipes, Heat Pumps, Refrigerators, Power Sources,"* Minsk, Belarus (2015), Vol. 2, pp. 4–11.
8. M. Habert and B. Agostini, Air to air thermosyphon heat exchanger for cabinet cooling, in: *Proc. 17th Int. Heat Pipe Conf.*, Kanpur, India (2013).